

Geophysical Research Letters®



RESEARCH LETTER

10.1029/2023GL107478

Key Points:

- Anomalous low Antarctic sea ice in austral winter amplifies upward planetary wave propagation in the spring, weakening the polar vortex
- Two climate models show the polar vortex weakening though it's only robust in one. This model has a negative Southern Annular Mode response
- Large polar vortex variability in early spring can mask the tropospheric circulation response to sea ice anomalies

Supporting Information:

Supporting Information may be found in the online version of this article.

Correspondence to:

A. H. Butler,
amy.butler@noaa.gov

Citation:

Rea, D., Elsbury, D., Butler, A. H., Sun, L., Peings, Y., & Magnusdottir, G. (2024). Interannual influence of Antarctic sea ice on Southern Hemisphere stratosphere-troposphere coupling. *Geophysical Research Letters*, 51, e2023GL107478. <https://doi.org/10.1029/2023GL107478>







Received 18 DEC 2023

Accepted 10 JUL 2024

© 2024 The Author(s). This article has been contributed to by U.S. Government employees and their work is in the public domain in the USA.

This is an open access article under the terms of the [Creative Commons Attribution-NonCommercial-NoDerivs License](#), which permits use and distribution in any medium, provided the original work is properly cited, the use is non-commercial and no modifications or adaptations are made.

Interannual Influence of Antarctic Sea Ice on Southern Hemisphere Stratosphere-Troposphere Coupling

Divya Rea¹ , Dillon Elsbury^{2,3} , Amy H. Butler² , Lantao Sun⁴ , Yannick Peings⁵ , and Gudrun Magnusdottir⁵ 

¹Department of Earth, Atmospheric, and Planetary Sciences, Massachusetts Institute of Technology, Cambridge, MA, USA, ²NOAA Chemical Sciences Laboratory, Boulder, CO, USA, ³Cooperative Institute for Research in Environmental Sciences, University of Colorado-Boulder, Boulder, CO, USA, ⁴Department of Atmospheric Science, Colorado State University, Fort Collins, CO, USA, ⁵Department of Earth System Science, University of California-Irvine, Irvine, CA, USA

Abstract While weakening of the boreal polar vortex may be caused by autumnal Arctic sea ice loss, less is known about the interannual influence of Antarctic sea ice on stratosphere-troposphere coupling in the Southern Hemisphere. Identifying any relationship over the short satellite period is difficult due to sampling variability and anthropogenic modification of the austral polar vortex. To circumvent these issues, we use large ensembles of fixed boundary condition simulations from the Community Atmosphere Model (CAM) and Whole Atmosphere Community Climate Model (WACCM) to assess if and how interannual fluctuations in winter Antarctic sea ice influence spring planetary-scale waves and the coupled stratosphere-troposphere circulation. Low Antarctic sea ice conditions are found to modulate tropospheric stationary waves to project constructively onto the climatological stationary wave, enhancing upward planetary wave propagation into the austral polar stratosphere. In WACCM, the resulting vortex weakening coincides with development of negative Southern Annular Mode conditions during September–November.

Plain Language Summary Antarctic sea ice concentrations vary from year to year, and the presence or lack of sea ice can change how the atmosphere above it responds. Here we use two specially designed experiments to understand how year to year variations in Antarctic sea ice affect the atmosphere from the surface to the stratosphere. We find that the winds in the stratosphere are slower than normal in years with less than normal sea ice. These changes in winds high up in the atmosphere may invoke changes in winds closer to the surface and in precipitation, but this result is model-dependent.

1. Introduction

Interactions between the stratosphere and troposphere are an important source of subseasonal to seasonal (S2S) predictability in the Southern Hemisphere (SH). Specifically, the strength of the stratospheric polar vortex in austral winter has been shown to influence the tropospheric circulation and surface impacts the following spring and summer (Lim et al., 2018). This stratosphere-troposphere coupling signal has been shown to be robust to sampling effects and predictable on S2S timescales (Byrne et al., 2019). However, understanding what factors drive interannual fluctuations in the austral polar vortex remains an open question.

In the Arctic, sea ice loss during Northern Hemisphere (NH) autumn has been associated with a weakening of the stratospheric polar vortex and an equatorward shift of the tropospheric jet stream in winter (Kim et al., 2014), but the response is strongly sensitive to the location of sea ice loss, as this influences how the atmospheric planetary wave response projects onto the climatological stationary wave pattern and amplifies into the stratosphere (McKenna et al., 2018; Sun et al., 2015). Other studies suggest that changes in Arctic sea ice only exert a small forcing on the polar vortex relative to the vortex's large internal variability (D. M. Smith et al., 2022), such that the polar vortex primarily contributes to substantial uncertainties in the tropospheric jet stream response (M. England et al., 2018; Peings et al., 2019; Sun et al., 2022).

In the Antarctic, the zonal-mean jet stream response to sea ice loss in general mirrors the response seen in the Arctic (M. England et al., 2018). Though one study found little impact on the tropospheric circulation in response to decreases in sea ice (Kidston et al., 2011), the imposed sea ice changes were highly idealized and the model used had a low model lid height, which may affect its ability to capture stratospheric variability (Charlton-Perez et al., 2013). Most other studies have found a robust weakening of the austral polar vortex in late autumn to winter

(M. England et al., 2018) or spring (H. H. Ayres & Screen, 2019), and a weakening of the tropospheric jet strength and negative Southern Annular Mode (SAM)-like surface response from austral winter to summer (H. Ayres & Screen, 2019; M. England et al., 2018; Menéndez et al., 1999; Raphael et al., 2011) in response to Antarctic sea ice loss. Similar to the Arctic (D. M. Smith et al., 2022), poorly simulated tropospheric eddy feedbacks have been linked to underestimated model responses of the tropospheric jet stream to sea ice perturbations (Screen et al., 2022).

Many of these studies impose large projected future losses in Antarctic sea ice in order to obtain a more robust circulation response. Less work has been done on the connection between sea ice concentration (SIC) and stratosphere-troposphere coupling in the Southern Hemisphere on interannual timescales. Anecdotal, two substantial weakenings of the spring polar vortex, so-called “sudden stratospheric warmings” (SSWs), that occurred in 2002 and 2019 were preceded by anomalously low winter sea ice extent. However, quantifying observed relationships may be difficult due to the relatively short period of satellite records (~40 yrs), slowly-evolving externally-forced changes to the polar vortex due to Antarctic ozone depletion which peaked in the late 20th century, and large atmospheric internal variability.

In this study, we use two different model large ensembles and methodologies to impose observed interannual fluctuations in Antarctic SIC, in order to determine whether there is a robust circulation response on interannual timescales to sea ice variability alone. We find that anomalously low sea ice in austral winter is associated with enhanced upward wave propagation and a weakening of the stratospheric polar vortex in spring. An associated equatorward shift of the springtime tropospheric jet stream and negative phase of the SAM is found, but only in one model; this model-dependence appears related to how well the model simulates stratosphere-troposphere coupling processes. Moreover, we find that the intrinsic variability of the polar vortex may contribute to uncertainties in the tropospheric and surface response, similarly to what has been shown for the NH.

2. Materials and Methods

We use version four of the Whole Atmosphere Community Climate Model (WACCM) (Marsh et al., 2013) and version six of the Community Atmosphere Model (CAM) (Danabasoglu et al., 2020). These models both have finite volume dynamical cores but different model physics. WACCM is a high-top model with 66 vertical levels, a model lid at 5.1×10^{-6} hPa, and a horizontal resolution of 1.9 latitude \times 2.5 longitude, whereas CAM is a low-top model with 32 vertical levels, a model lid at 3.64 hPa, and a higher horizontal resolution of 0.9 latitude \times 1.25 longitude. Both models were run with specified chemistry in which time-averaged 1995–2005 zonal-mean monthly (WACCM) and 5-day averaged (CAM) ozone climatologies and mean chemical and shortwave heating rates are prescribed (K. L. Smith et al., 2014).

For WACCM, two 10-member ensembles are run with fixed year 2000 radiative forcing. The first ensemble is forced with atmospheric model intercomparison project (AMIP) style boundary conditions, with prescribed chronologies of 1978–2016 sea surface temperature and SIC (Hadley Center Sea Ice and Sea Surface Temperature, HadISST, Rayner et al. (2003)) and a prescribed Quasi-biennial Oscillation (QBO) via nudging of the tropical stratospheric winds. The second ensemble has identical boundary conditions and prescribed QBO as the first, however the SIC forcing is a repeating annual cycle of climatological SIC rather than the full chronology; this is the “AMIP-climSIC” experiments as defined for the Polar Amplification Model Intercomparison Project (PAMIP) (D. M. Smith et al., 2019). Both ensembles were originally run for PAMIP and more details can be found in (D. M. Smith et al., 2019). After deseasonalizing the AMIP and AMIP-climSIC ensemble members, their difference is taken for each member, and then the differences are averaged across members, thereby isolating the atmospheric response to the 1978–2016 SIC chronology. This atmospheric response is then subsampled for low and high Antarctic SIC years, years during which the July SIC (latitudinally averaged with cosine-weighting 55°S–90°S) is less than -1 or greater than $+1$ standard deviation from the full 1978–2016 climatology. The sensitivity of the results to SIC in months other than July is discussed in Section 3. Statistical significance for the AMIP versus AMIP-climSIC anomalies is assessed by using the bootstrapped student's *t*-test of Efron and Tibshirani (1994, algorithm, 16.2). Statistical significance for WACCM's low (high) SIC composites are assessed by comparing the AMIP and AMIP-climSIC samples during low (high) SIC years. Statistical significance for WACCM's composite differences are assessed by comparing the anomalies during low SIC years to those during high SIC years. P-values <0.05 are deemed statistically significant.

There is a somewhat different experimental set up in the CAM simulations. For CAM, there are two 8-member ensembles run with fixed year 2000 radiative forcing, repeating annual cycles of time-averaged 1978–2019 climatological SSTs, and the 1978–2019 chronology of SIC from HadISST. The only difference between the two 8-member ensembles is their Arctic sea ice thicknesses; 2-m in one ensemble versus Pan-Arctic Ice Ocean Modeling and Assimilation System (PIOMAS) observations in the other. The Antarctic sea ice thickness is set to 1-m everywhere in both ensembles. Since we are only concerned with Antarctic sea ice in this study, we combine the two 8-member ensembles into one 16-member ensemble. Anomalies in this combined ensemble are defined as deviations from the seasonal cycle (defined for each member), and composites of those anomalies during the same low and high July Antarctic SIC years as used for WACCM are shown. Since the CAM simulations are 3 yrs longer than the WACCM simulations, only the common 1978–2016 period is considered (results are nearly identical if the longer period is used for CAM). Statistical significance is determined again using the bootstrapped student's *t*-test (cases when $p < 0.05$). Statistical significance for CAM's low and high SIC anomalies, respectively, is computed by comparing each to the anomalies from neutral SIC years (between +1 and −1 stdev). Statistical significance for CAM's low minus high SIC composite is assessed by comparing the respective anomalies.

ERA5 data (Hersbach et al., 2020) from 1978 to 2016 is shown in some supplemental figures. Because Antarctic ozone depletion and recovery strongly influenced the strength of the springtime polar vortex, the timing of its seasonal transition, and its coupling to the surface during this time period, we regress out the signal related to the long-term evolution of ozone-depleting substances (Figure S1 in Supporting Information S1, Newman et al., 2007) from the ERA5 zonal-mean zonal wind, though this step doesn't qualitatively change the results.

3. Results

The relationship between winter Antarctic sea ice and stratosphere-troposphere coupling over the period of satellite records (1978–2016) in ERA5 reanalysis suggests weakening of the spring vortex during low SIC compared to high SIC winters, which is qualitatively insensitive to the threshold of SIC anomaly chosen (Figure S2 in Supporting Information S1). However, the zonal wind differences between low and high SIC winters are generally not statistically significant. Other sources of interannual variability, such as the El Niño-Southern Oscillation (Stone et al., 2021) or the QBO (Rao et al., 2023), also influence SH springtime stratosphere-troposphere coupling, so that detecting the influence of sea ice fluctuations may be obscured, particularly given sampling limitations in the short satellite record. Therefore, to isolate the atmospheric circulation response to SIC interannual variability, we turn to the two large ensemble experiments described in Section 2.

We focus on SIC variations in austral winter, when an exposed ocean surface can rapidly lose heat to the atmosphere and the surface heat flux response maximizes (M. England et al., 2018). We explored various fall to winter SIC indices, including April, May, June, July, and August plus their combinations (e.g., MJ, JJA). Years for which SIC fell below −1 or above +1 standard deviation are generally similar when using May through August-based indices (Figure 1a), reflecting the persistence of the SIC state through winter. We use the July SIC index in the rest of our analysis to represent the state of the austral winter SIC anomalies; atmospheric composite responses shown in Figures 2–4 are qualitatively similar no matter which SIC index is selected (not shown). There are 6 yrs of anomalously low July SIC and 6 yrs of anomalously high July SIC (Figure 1a). Because we are using large ensembles, the total sample size for, for example, low SIC years, will be 6 yrs multiplied by the number of ensemble members in WACCM (10) and CAM (16). Note that the apparent jump in SIC around 2009–2011 has been linked to a change in observation system in HadISST (Screen, 2011), so may not accurately reflect observed variability; nonetheless since this feature was part of the model boundary forcing, the simulated atmospheric response should still be consistent with high SIC during those years. Using only the 1979–2008 period gave qualitatively the same atmospheric responses shown here.

During low July SIC years, the largest negative SIC anomalies in July occur over the Amundsen and Ross Seas (130°W) and the Indian Ocean sector (20°E) (Figure 1b). The negative SIC anomaly over the Indian Ocean disappears after August, while the negative SIC anomaly over the Amundsen and Ross Seas expands eastward over time, with some positive SIC anomalies appearing west of the Ross Sea during September and October (Figures 1c–1e). Previous studies have shown that anomalies in SIC and associated surface heat fluxes can drive asymmetrical responses in atmospheric pressure, influencing planetary-scale atmospheric wave patterns (Woollings et al., 2023). The sea level pressure (SLP) anomalies composited for low July SIC years in WACCM

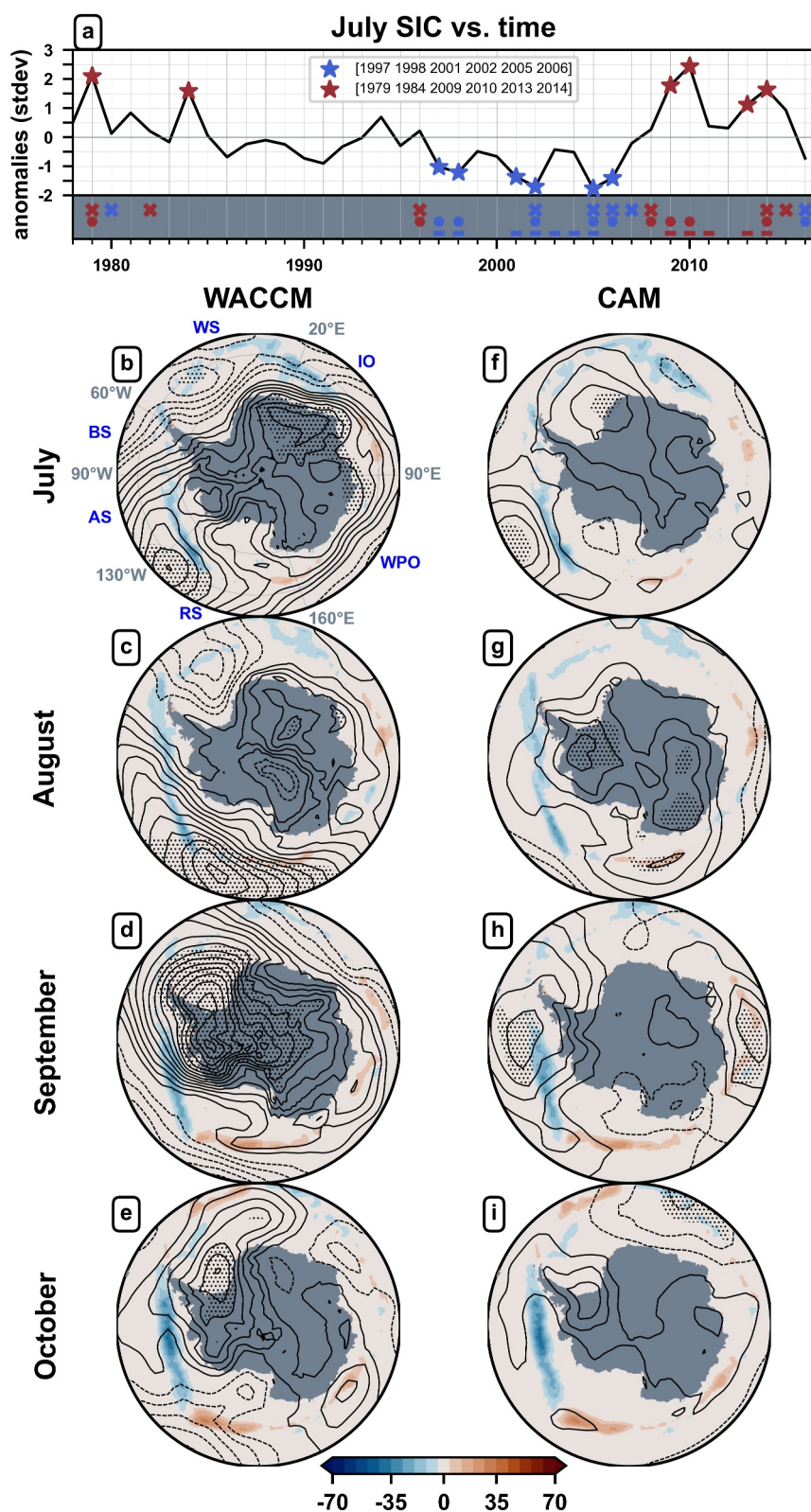


Figure 1.

(Figures 1b–1e) shows anomalously high SLP over the Amundsen and Ross Seas that overlies the region of persistent sea ice loss there. This region of anomalously high SLP generally moves eastward from July to October as the region of negative SIC anomaly also expands eastward. Anomalously low SLP over the Antarctic Peninsula and Weddell Seas in July also moves eastward into spring, ending up at the Indian Ocean sector by October. In CAM (Figures 1f–1i), the composited SLP responses to low July SIC are much weaker than in WACCM, though the anomalously high SLP over the Amundsen Sea that forms in July and shifts eastward in the following months is similar spatially. The SLP anomalies for low SIC years in ERA5 (Figures S3b–S3e in Supporting Information S1), while subject to sampling variability, also highlight the eastward movement of the high SLP anomaly that maximizes in September over the Antarctic peninsula.

The sea ice anomaly composite for high July SIC (Figure S4 in Supporting Information S1) by construction shows generally an opposite-signed response to low July SIC, but the spatial pattern is not a perfect mirror image. Unlike for low SIC years, the high SIC anomalies in the Indian Ocean sector are of near equal amplitude to those in the Amundsen/Ross Seas and persist from July–October. The corresponding composite SLP anomalies for high July SIC (Figure S4 in Supporting Information S1) generally show an anomalous trough overlying positive ice anomalies in the Amundsen Sea in July–August that shifts eastward by September–October. However, WACCM shows the September–October anomalous trough further north and east compared to CAM, which instead places it over the Antarctic peninsula. Neither model shows a clear opposite-signed (linear) atmospheric response between low and high SIC years. Because of these apparent non-linearities in both the sea ice forcing and the atmospheric response, we show responses to low and high SIC years separately.

Moving upward from the surface forcing, in low July SIC years an anomalous tropospheric ridge over the Amundsen/Ross Seas in both models, and an anomalous trough over the Weddell Sea in WACCM, forms in July and drifts eastward over the next months (Figures S5 and S6 in Supporting Information S1). By September–October, the anomalous ridge over the Antarctic peninsula is in the right location to reinforce the climatological ridge (Figures 2a and 2d). In WACCM (Figure 2a), the anomalous trough that has shifted to the Indian Ocean sector (20–90°E) by September–October also reinforces the climatological trough while in CAM (Figure 2d), this component is largely absent. During high July SIC years, in WACCM there is an eastward propagation of an anomalous trough from the Amundsen Sea to the Weddell Sea that leads to destructive interference with the climatological wave pattern (Figure 2b, Figure S5 in Supporting Information S1; note that the pattern does not persist into October so the destructive interference is less obvious in Figure 2b which averages September–October). In CAM, the anomalous trough does not move as far eastward as in WACCM (Figure S6 in Supporting Information S1), and so it projects roughly in quadrature to the climatological wave pattern (Figure 2e).

The differences in the atmospheric planetary-wave response between WACCM and CAM may arise for a number of reasons. First, WACCM shows a more baroclinic (westward-tilting) response with height, while CAM's response is more barotropic (vertically stacked). This might be related to differences in the climatological stationary waves between the models, as CAM also shows less “tilt” climatologically (Figures 2a and 2d). There is also a difference in the timing/evolution of the response, particularly in high SIC years; in CAM, the atmospheric responses that start in the Amundsen sea in July do not propagate eastward as quickly as in WACCM, so that the SLP and eddy height responses match more closely to the response in WACCM a month later (Figures S5 and S6 in Supporting Information S1). While it is difficult to diagnose the exact reasons for the model differences, the end result is that in WACCM the large-scale wave response much more strongly constructively interferes with the climatological wave pattern compared to CAM in both low and high SIC years (Figure 2).

Constructive linear interference corresponds to amplification of the wave vertically into the stratosphere, associated with poleward eddy heat fluxes— which are climatologically negative in the SH. In both models low (high) SIC years are associated with anomalously poleward (equatorward) eddy heat fluxes from 100 to 10 hPa that peak

Figure 1. (a) Time series of standardized longitudinally and latitudinally averaged 55°S–90°S July sea ice concentration (SIC) anomalies, with low and high (± 1 standard deviation) years denoted by blue and red stars, respectively. The gray region beneath the time series shows what low/high SIC years would comprise the index if it was instead defined using May (crosses), June (filled circles), or August (horizontal lines). (b–i) Red and blue shading shows percent change in July to October SIC relative to climatology during low July SIC years. Sea level pressure (SLP) anomalies in (b–e) WACCM and (f–i) CAM are contoured in black with ± 0.25 hPa intervals. Stippling denotes statistically significant SLP anomalies, calculated as in Methods. Southern Ocean sectors mentioned in this study are labeled on (b) in a manner consistent with Turner et al. (2016): Weddell Sea (WS), Indian Ocean (IO), Western Pacific Ocean (WPO), Ross Sea (RS), Amundsen Sea (AS), and Bellingshausen Sea (BS).

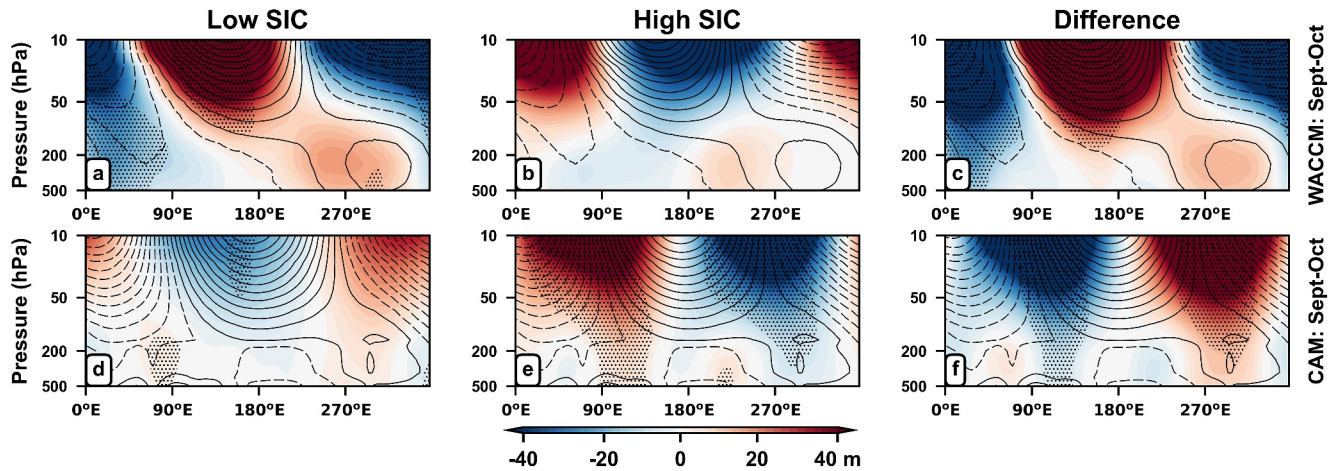


Figure 2. (a–c) Pressure–longitude cross-section of anomalous (shading) September–October (a–c) WACCM and (d–f) CAM eddy geopotential heights latitudinally averaged between 60°S and 90°S. Stippling denotes statistically significant anomalies (methods). Each model's climatological eddy geopotential height is contoured in black with intervals of ± 50 m with the first solid and negative black contours corresponding to 25 and -25 m, respectively. Composites are shown for (a and d) low sea ice concentration (SIC) years, (b and e) high SIC years, and (c and f) low minus high SIC years.

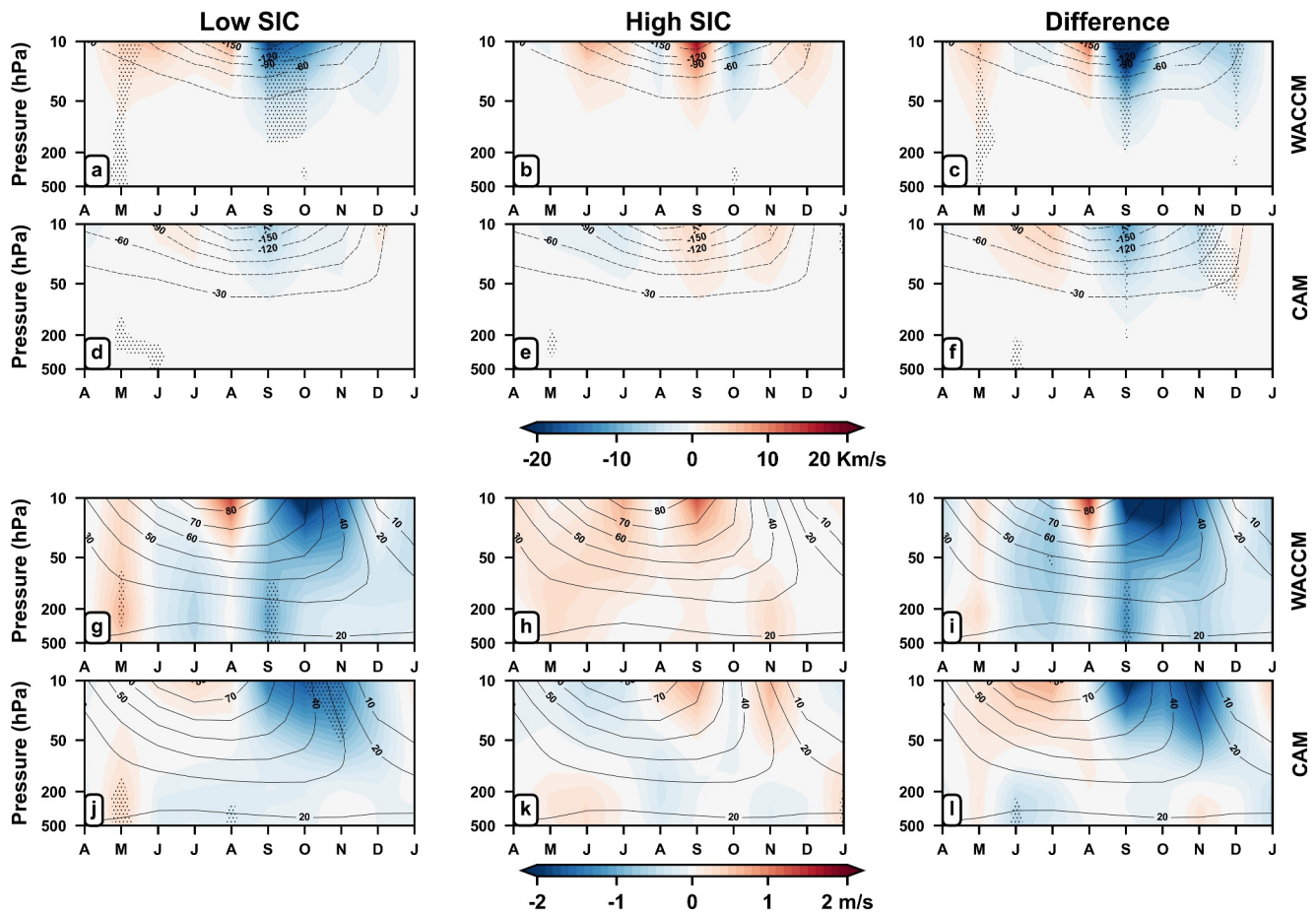


Figure 3. Pressure–month cross-sections of anomalous (a–c) WACCM and (d–f) CAM longitudinally and latitudinally averaged 60°S–90°S eddy heat flux anomalies. Stippling denotes statistically significant anomalies (methods). Each model's climatological eddy heat flux is contoured in black with intervals of ± 30 Km/s. Composites are shown for (a and d) low SIC years, (b and e) high SIC years, and (c and f) low minus high SIC years. (g–l) Same as (a–f), but for 50°S–70°S zonal wind with the black climatological contours having intervals of 10 m/s.

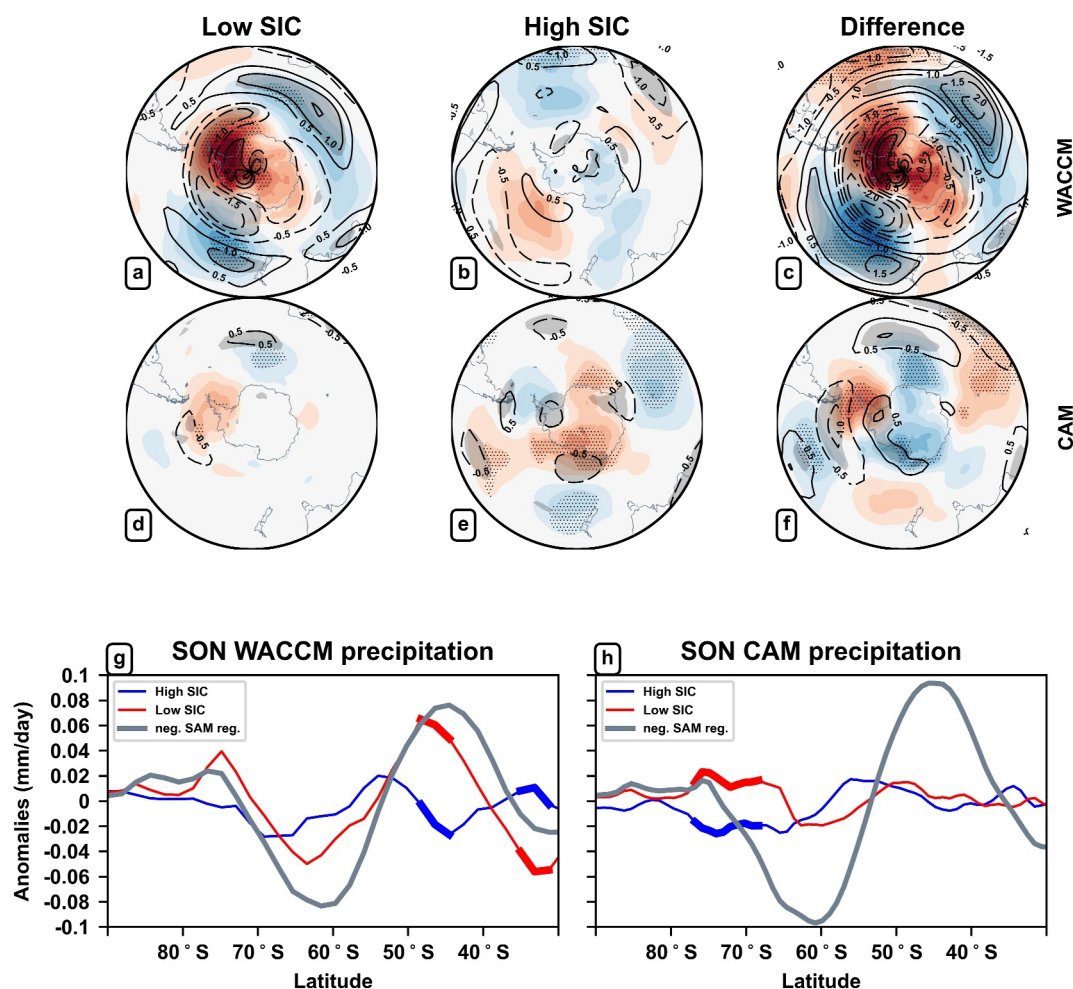


Figure 4. Composites SON sea level pressure (SLP) anomalies (shading) and 200 hPa zonal wind anomalies (contours) for (a and d) low July sea ice concentration (SIC) years, (b and e) high July SIC years, and (c and f) low minus high SIC composite differences. Results from WACCM are shown in panels a–c and from CAM in panels d–f. Statistical significance for (a–c) and (d–f) is the same as Figures 3a–3f and is denoted by stippling for the SLP and by gray undershading for the zonal winds. (g and h) Zonal-mean precipitation anomalies for high (blue) and low (red) July SIC years, with thicker curves denoting statistical significance, and the gray curve denoting precipitation regressed onto the model's negative SAM index (defined as in Gong and Wang (1999)), for (g) WACCM and (h) CAM.

around September, but this response is much stronger in WACCM (Figures 3a–3f). The delayed timing between the July SIC forcing and the upward propagation of heat flux in September can be linked to: (a) the time for the sea ice forcing to shift eastward, and for the atmospheric wave response to line up with the climatological wave pattern, and (b) to the time of year when the polar vortex climatologically begins to weaken, allowing anomalies in tropospheric wave forcing to interact more strongly with the stratospheric mean flow (Lim et al., 2018).

The increased vertical wave propagation into the stratosphere during September–October in low July SIC years acts to disrupt and weaken the polar vortex (Figures 3g–3l). Both WACCM and CAM indicate that low SIC years are associated with a negative zonal wind anomaly from 50 to 70°S (on the poleward side of the climatological jet maximum) that is largest in magnitude in the stratosphere and extends downward to the surface from September–December (Figures 3g and 3j). Additionally, in WACCM low July SIC yields a positive tropospheric zonal mean zonal wind anomaly during September–November around 45°S (not shown), corresponding to an equatorward shift of the tropospheric jet and the negative phase of the SAM. During high July SIC years the response is roughly opposite in sign but weaker in magnitude (Figures 3h and 3k). The zonal wind responses in CAM are qualitatively similar to WACCM but are generally weaker in magnitude at 10 hPa; perhaps as a consequence, the zonal wind anomalies exhibit less downward descent from the stratosphere to the surface during October–December

(Figures 3j–3l). To understand whether this reduced stratosphere-troposphere coupling in CAM relative to WACCM is related to systematic model biases, Figure S7 in Supporting Information S1 shows a metric of stratosphere-troposphere coupling for each ensemble member of WACCM and CAM across the entire time series (irrespective of low or high sea ice years). CAM systematically underestimates the coupling of the stratosphere to the troposphere compared to ERA5, but WACCM systematically overestimates the coupling. Therefore the magnitude of the downward stratosphere-troposphere coupling anomalies to low July SIC years found here likely falls somewhere in between what is found for WACCM and CAM.

An early weakening of the austral polar vortex has previously been shown to have a downward influence on the troposphere, with negative SAM conditions that can increase risk of hot and dry extremes in southeastern Australia in late spring to summer (Lim et al., 2019). In agreement with the weakened polar vortex and equatorward shift of the tropospheric jet response to low SIC years in WACCM (Figure 3g), we find a significant negative SAM-like response in SLP during September–November, with anomalously high SLP over Antarctica and anomalously low SLP over the Pacific and Atlantic sectors of the Southern Ocean (Figure 4a). The eddy-driven jet weakens over the coast of Antarctica and strengthens over much of the mid-latitude Southern Ocean. Some of these SLP and upper-level tropospheric jet features are roughly opposite in sign during high SIC years, but are not statistically significant (Figure 4b). Conversely, CAM yields no significant September–November SLP or eddy-driven jet responses following either low or high July SIC (Figures 4d and 4e). WACCM and CAM also yield contrasting September–November precipitation responses (Figures 4g and 4h). WACCM exhibits a positive anomaly between 40 and 50°S and a negative anomaly near 30°S during low SIC years (which projects well onto the negative SAM pattern), with weaker but opposite-signed responses during high SIC years (Figure 4g). In CAM, significant differences in precipitation between low and high SIC years only occur closer to the pole at 70–75°S (Figure 4h), and do not resemble the SAM signature, which is consistent with the lack of SAM response in CAM.

While the negative SAM response in WACCM is consistent with a weakened polar vortex and downward coupling, it is possible that this tropospheric signal arises not only from the stratospheric influence but some other pathway of the SIC influence on the SAM (Bader et al., 2013; Raphael et al., 2011). Indeed, Figures 3g and 3j shows that in both WACCM and CAM the tropospheric zonal winds weaken during austral winter in response to low July SIC, prior to the stratospheric response. However, the response in the stratosphere lasts throughout spring in both WACCM and CAM, and may contribute to the persistence of the coupling between winter sea ice anomalies and spring to summer circulation patterns.

Previous studies have suggested that the internal variability of the Arctic stratospheric polar vortex could contribute to uncertainties in the signal of Arctic sea ice loss on the tropospheric circulation (M. England et al., 2018; Peings et al., 2019; Sun et al., 2022). Similarly, internal variability of the austral polar vortex can mask the interannual tropospheric response to Antarctic sea ice (Figure S8 in Supporting Information S1). Looking at WACCM for low July SIC years, we can find individual ensemble members with a weaker or stronger polar vortex (AMIP vs. AMIP-climSIC difference) in July–August (Figure S8 in Supporting Information S1, columns 1 and 2); there is large spread even for the same SIC forcing. Grouping members by the strength of the vortex difference in July–August shows that the initial strength of the vortex dominates the evolution of the September–November tropospheric zonal-mean zonal wind response to low July SIC years. Only in the ensemble-mean, when we average over many samples to damp the noise, do we see the responses to low SIC in Figure 3. As is the case for many seasonal predictors, this analysis suggests that large forecast ensembles may be needed to predict probabilistic shifts in the atmospheric circulation due to sea ice variability during any given year.

4. Discussion

Using model experiments well suited to isolate the atmospheric response to the observed chronology of austral SIC, we find that anomalously low sea ice in austral winter is associated with the development of a planetary-scale wave pattern in the troposphere by September characterized by a ridge over the Antarctic Peninsula. This ridge has also been shown to exist during the 10% of strongest upward planetary wave propagation events in the SH (M. R. England et al., 2016). This wave pattern constructively interferes with the climatological wave pattern, leading to upward wave propagation and a disruption of the stratospheric circulation into late spring. Opposite-signed responses are generally apparent in response to high sea ice, but it is also evident that the

atmospheric response is not linear, in part because the sea ice forcing itself is not linear spatially between high and low sea ice years.

This signal was detected using large ensembles of both WACCM and CAM, indicating that it is not attributable to noise, and the mechanism is similar to that found in the Arctic (Kim et al., 2014) and in response to projected future Antarctic sea ice loss (H. H. Ayres & Screen, 2019; M. England et al., 2018). In WACCM only, the weakened springtime polar vortex response to low SIC years is consistent with a negative SAM, enhanced mid-latitude precipitation, and reduced subtropical precipitation. The lack of surface response in CAM may simply stem from the weaker stratospheric response in CAM to sea ice forcing, but a comparison of climatological stratosphere-troposphere coupling strength in WACCM and CAM compared to ERA5 suggests that WACCM is likely overestimating the stratosphere-troposphere coupling response while CAM is underestimating it. Differences in WACCM's and CAM's responses may also stem, in part, from differences in experimental setup, for instance how the anomalies are calculated within either ensemble, or how WACCM uses AMIP SSTs while CAM uses climatological SSTs.

Because this study focuses on the effect of interannual variability in SIC on the atmospheric circulation, the atmospheric response may be smaller in magnitude than studies which prescribe larger future SIC changes. However, the benefit of this methodology is that the experiments are designed to quantify the extent to which realistic interannual variations in SIC could contribute to predictable shifts in the strength of stratosphere-troposphere coupling for any given year. Understanding the factors that influence the strength of the spring austral polar vortex may allow for better prediction of (a) the size of the Antarctic ozone hole which is strongly linked to polar vortex strength on interannual timescales (Salby et al., 2012) and (b) austral surface climate in late spring to early summer (Lim et al., 2018). Our results suggest that a large sample size is needed to detect the signal of SIC anomalies on the atmospheric circulation given the large variability of the stratosphere and troposphere (e.g., Peings et al. (2021)). Note, however, that neither model used here includes interactive stratospheric chemistry. Any feedbacks between stratospheric ozone and the strength of the polar vortex, which have been found to enhance the surface impact (Li et al., 2016), are thus not captured. There is also no ocean-atmosphere coupling in either model used in this study. A coupled ocean was found to amplify the atmospheric circulation response to Arctic SIC loss (Deser et al., 2015) and to Antarctic SIC loss (H. C. Ayres et al., 2022; D. M. Smith et al., 2017). In general, the lack of coupling to chemistry and the ocean in our study implies that the responses to SIC documented here are likely underestimated, though the combined influence of different couplings on the response may not be straightforward (Gillett et al., 2019).

Although Antarctic SIC has shown an overall increasing trend over the satellite record, between 2014 and 2023, SIC dropped from a record high to record low, with the 2023 SIC anomaly falling well below any previously observed anomaly. Interestingly, substantial poleward heat fluxes were evident throughout July and August 2023 and a minor SSW occurred in September 2023, in agreement with the mechanism described in this study. While further work needs to be done to attribute these circulation changes to the record low Antarctic SIC, this unexpected dramatic melting may portend a new regime of low Antarctic sea ice (Eayrs et al., 2021; Purich & Doddridge, 2023). Understanding the complexities of how Antarctic sea ice variability interacts with the atmospheric circulation as the climate warms and the ozone layer recovers may offer insights into how to improve seasonal prediction of Southern Hemisphere surface climate.

Data Availability Statement

All data used to produce figures in the main manuscript from WACCM4 and CAM6 models is publicly available at Elsberry et al. (2024).

References

- Ayres, H., & Screen, J. (2019). Multimodel analysis of the atmospheric response to Antarctic Sea Ice loss at quadrupled CO₂. *Geophysical Research Letters*, 46(16), 9861–9869. <https://doi.org/10.1029/2019GL083653>
- Ayres, H. C., Screen, J. A., Blockley, E. W., & Bracegirdle, T. J. (2022). The coupled atmosphere–ocean response to Antarctic Sea Ice loss. *Journal of Climate*, 35(14), 4665–4685. <https://doi.org/10.1175/JCLI-D-21-0918.1>
- Bader, J., Flügge, M., Kvamstø, N. G., Mesquita, M. D. S., & Voigt, A. (2013). Atmospheric winter response to a projected future Antarctic sea-ice reduction: A dynamical analysis. *Climate Dynamics*, 40(11), 2707–2718. <https://doi.org/10.1007/s00382-012-1507-9>
- Byrne, N. J., Shepherd, T. G., & Polichtchouk, I. (2019). Subseasonal-to-Seasonal predictability of the Southern Hemisphere eddy-driven jet during austral spring and early summer. *Journal of Geophysical Research: Atmospheres*, 124(13), 6841–6855. <https://doi.org/10.1029/2018JD030173>

Acknowledgments

We appreciate support from the Ernest F. Hollings Undergraduate Scholarship Program. We acknowledge the World Climate Research Programme, which, through its Polar Amplification Modelling Intercomparison Project, coordinated and promoted the experiments used herein. We would like to acknowledge high-performance computing support from Cheyenne <https://doi.org/10.5065/D6RX99HX> provided by NCAR's Computational and Information Systems Laboratory, sponsored by the National Science Foundation.

- Charlton-Perez, A. J., Baldwin, M. P., Birner, T., Black, R. X., Butler, A. H., Calvo, N., et al. (2013). On the lack of stratospheric dynamical variability in low-top versions of the CMIP5 models. *Journal of Geophysical Research: Atmospheres*, 118(6), 2494–2505. <https://doi.org/10.1002/jgrd.50125>
- Danabasoglu, G., Lamarque, J.-F., Bacmeister, J., Bailey, D. A., DuVivier, A. K., Edwards, J., et al. (2020). The Community Earth System Model version 2 (CESM2). *Journal of Advances in Modeling Earth Systems*, 12(2), e2019MS001916. <https://doi.org/10.1029/2019MS001916>
- Deser, C., Tomas, R. A., & Sun, L. (2015). The role of ocean–atmosphere coupling in the zonal-mean atmospheric response to arctic Sea Ice loss. *Journal of Climate*, 28(6), 2168–2186. <https://doi.org/10.1175/JCLI-D-14-00325.1>
- Eayrs, C., Li, X., Raphael, M. N., & Holland, D. M. (2021). Rapid decline in Antarctic sea ice in recent years hints at future change. *Nature Geoscience*, 14(7), 460–464. <https://doi.org/10.1038/s41561-021-00768-3>
- Efron, B., & Tibshirani, R. J. (1994). *An introduction to the bootstrap* (1st ed.). Chapman and Hall/CRC. <https://doi.org/10.1201/9780429246593>
- Elsbury, D., Peings, Y., & Sun, L. (2024). Data for Interannual influence of Antarctic sea ice on Southern Hemisphere stratosphere-troposphere coupling [Dataset]. *OSF*. <https://doi.org/10.17605/OSF.IO/RHQBVB>
- England, M., Polvani, L., & Sun, L. (2018). Contrasting the Antarctic and Arctic atmospheric responses to projected sea ice loss in the late 21st Century. *Journal of Climate*, 31(16), 6353–6370. <https://doi.org/10.1175/JCLI-D-17-0666.1>
- England, M. R., Shaw, T. A., & Polvani, L. M. (2016). Troposphere–stratosphere dynamical coupling in the southern high latitudes and its linkage to the Amundsen Sea. *Journal of Geophysical Research: Atmospheres*, 121(8), 3776–3789. <https://doi.org/10.1002/2015JD024254>
- Gillett, Z. E., Arblaster, J. M., Dittus, A. J., Deushi, M., Jöckel, P., Kinnison, D. E., et al. (2019). Evaluating the relationship between interannual variations in the Antarctic Ozone Hole and Southern Hemisphere surface climate in chemistry–climate models. *Journal of Climate*, 32(11), 3131–3151. <https://doi.org/10.1175/JCLI-D-18-0273.1>
- Gong, D., & Wang, S. (1999). Definition of Antarctic Oscillation index. *Geophysical Research Letters*, 26(4), 459–462. <https://doi.org/10.1029/1999gl900003>
- Hersbach, H., Bell, B., Berrisford, P., Hirahara, S., Horányi, A., Muñoz-Sabater, J., et al. (2020). The ERA5 global reanalysis. *Quarterly Journal of the Royal Meteorological Society*, 146(730), 1999–2049. <https://doi.org/10.1002/qj.3803>
- Kidston, J., Taschetto, A. S., Thompson, D. W. J., & England, M. H. (2011). The influence of Southern Hemisphere sea-ice extent on the latitude of the mid-latitude jet stream. *Geophysical Research Letters*, 38(15), L15804. <https://doi.org/10.1029/2011GL048056>
- Kim, B.-M., Son, S.-W., Min, S.-K., Jeong, J.-H., Kim, S.-J., Zhang, X., et al. (2014). Weakening of the stratospheric polar vortex by Arctic sea-ice loss. *Nature Communications*, 5(1), 4646. <https://doi.org/10.1038/ncomms5646>
- Li, F., Vikhliav, Y. V., Newman, P. A., Pawson, S., Perlwitz, J., Waugh, D. W., & Douglass, A. R. (2016). Impacts of interactive stratospheric chemistry on Antarctic and Southern Ocean climate change in the Goddard Earth Observing System—version 5 (GEOS-5). *Journal of Climate*, 29(9), 3199–3218. <https://doi.org/10.1175/JCLI-D-15-0572.1>
- Lim, E.-P., Hendon, H. H., Boschat, G., Hudson, D., Thompson, D. W. J., Dowdy, A. J., & Arblaster, J. M. (2019). Australian hot and dry extremes induced by weakenings of the stratospheric polar vortex. *Nature Geoscience*, 12(11), 896–901. <https://doi.org/10.1038/s41561-019-0456-x>
- Lim, E.-P., Hendon, H. H., & Thompson, D. W. J. (2018). Seasonal evolution of stratosphere-troposphere coupling in the southern Hemisphere and implications for the predictability of surface climate. *Journal of Geophysical Research: Atmospheres*, 123(21), 12002–12016. <https://doi.org/10.1029/2018JD029321>
- Marsh, D. R., Mills, M. J., Kinnison, D. E., Lamarque, J.-F., Calvo, N., & Polvani, L. M. (2013). Climate change from 1850 to 2005 simulated in CESM1(WACCM). *Journal of Climate*, 26(19), 7372–7391. <https://doi.org/10.1175/JCLI-D-12-00558.1>
- McKenna, C. M., Bracegirdle, T. J., Shuckburgh, E. F., Haynes, P. H., & Joshi, M. M. (2018). Arctic Sea ice loss in different regions leads to contrasting Northern Hemisphere impacts. *Geophysical Research Letters*, 45(2), 945–954. <https://doi.org/10.1002/2017GL076433>
- Menéndez, C. G., Serafini, V., & Le Treut, H. (1999). The effect of sea-ice on the transient atmospheric eddies of the Southern Hemisphere. *Climate Dynamics*, 15(9), 659–671. <https://doi.org/10.1007/s003820050308>
- Newman, P. A., Daniel, J. S., Waugh, D. W., & Nash, E. R. (2007). A new formulation of Equivalent Effective Stratospheric Chlorine (EESC). *Atmospheric Chemistry and Physics*, 7(17), 4537–4552. <https://doi.org/10.5194/acp-7-4537-2007>
- Peings, Y., Cattiaux, J., & Magnusdottir, G. (2019). The polar stratosphere as an arbiter of the projected tropical versus polar tug of war. *Geophysical Research Letters*, 46(15), 9261–9270. <https://doi.org/10.1029/2019GL082463>
- Peings, Y., Labe, Z. M., & Magnusdottir, G. (2021). Are 100 ensemble members enough to capture the remote atmospheric response to +2°C Arctic Sea Ice loss? *Journal of Climate*, 34(10), 3751–3769. <https://doi.org/10.1175/JCLI-D-20-0613.1>
- Purich, A., & Doddridge, E. W. (2023). Record low Antarctic sea ice coverage indicates a new sea ice state. *Communications Earth & Environment*, 4(1), 1–9. <https://doi.org/10.1038/s43247-023-00961-9>
- Rao, J., Garfinkel, C. I., Ren, R., Wu, T., & Lu, Y. (2023). Southern Hemisphere response to the quasi-biennial oscillation in the CMIP5/6 models. *Journal of Climate*, 1(8), 1–45. <https://doi.org/10.1175/JCLI-D-22-0675.1>
- Raphael, M. N., Hobbs, W., & Wainer, I. (2011). The effect of Antarctic sea ice on the Southern Hemisphere atmosphere during the southern summer. *Climate Dynamics*, 36(7), 1403–1417. <https://doi.org/10.1007/s00382-010-0892-1>
- Rayner, N. A., Parker, D. E., Horton, E. B., Folland, C. K., Alexander, L. V., Rowell, D. P., et al. (2003). Global analyses of sea surface temperature, sea ice, and night marine air temperature since the late nineteenth century. *Journal of Geophysical Research*, 108(D14), 4407. <https://doi.org/10.1029/2002JD002670>
- Salby, M. L., Titova, E. A., & Deschamps, L. (2012). Changes of the Antarctic ozone hole: Controlling mechanisms, seasonal predictability, and evolution. *Journal of Geophysical Research*, 117(D10), D10111. <https://doi.org/10.1029/2011JD016285>
- Screen, J. A. (2011). Sudden increase in Antarctic sea ice: Fact or Artifact? *Geophysical Research Letters*, 38(13). <https://doi.org/10.1029/2011GL047553>
- Screen, J. A., Eade, R., Smith, D. M., Thomson, S., & Yu, H. (2022). Net equatorward shift of the jet streams when the contribution from sea-ice loss is constrained by observed eddy feedback. *Geophysical Research Letters*, 49(23), e2022GL100523. <https://doi.org/10.1029/2022GL100523>
- Smith, D. M., Dunstone, N. J., Scaife, A. A., Fiedler, E. K., Copsey, D., & Hardiman, S. C. (2017). Atmospheric response to Arctic and Antarctic sea ice: The importance of ocean-atmosphere coupling and the background state. *Journal of Climate*, 30(12), 4547–4565. <https://doi.org/10.1175/JCLI-D-16-0564.1>
- Smith, D. M., Eade, R., Andrews, M. B., Ayres, H., Clark, A., Chripko, S., et al. (2022). Robust but weak winter atmospheric circulation response to future Arctic sea ice loss. *Nature Communications*, 13(1), 727. <https://doi.org/10.1038/s41467-022-28283-y>
- Smith, D. M., Screen, J. A., Deser, C., Cohen, J., Fyfe, J. C., García-Serrano, J., et al. (2019). The Polar Amplification Model Intercomparison Project (PAMIP) contribution to CMIP6: Investigating the causes and consequences of polar amplification. *Geoscientific Model Development*, 12(3), 1139–1164. <https://doi.org/10.5194/gmd-12-1139-2019>

- Smith, K. L., Neely, R. R., Marsh, D. R., & Polvani, L. M. (2014). The specified chemistry Whole Atmosphere Community Climate Model (SC-WACCM). *Journal of Advances in Modeling Earth Systems*, 6(3), 883–901. <https://doi.org/10.1002/2014MS000346>
- Stone, K. A., Solomon, S., Thompson, D. W. J., Kinnison, D. E., & Fyfe, J. C. (2021). On the Southern Hemisphere stratospheric response to ENSO and its impacts on tropospheric circulation. *Journal of Climate*, 35(6), 1–51. <https://doi.org/10.1175/JCLI-D-21-0250.1>
- Sun, L., Deser, C., Simpson, I., & Sigmond, M. (2022). Uncertainty in the winter tropospheric response to Arctic Sea ice loss: The role of stratospheric polar vortex internal variability. *Journal of Climate*, 35(10), 1–58. <https://doi.org/10.1175/JCLI-D-21-0543.1>
- Sun, L., Deser, C., & Tomas, R. A. (2015). Mechanisms of stratospheric and tropospheric circulation response to projected Arctic Sea Ice loss. *Journal of Climate*, 28(19), 7824–7845. <https://doi.org/10.1175/JCLI-D-15-0169.1>
- Turner, J., Hosking, J. S., Marshall, G. J., Phillips, T., & Bracegirdle, T. J. (2016). Antarctic sea ice increase consistent with intrinsic variability of the Amundsen Sea Low. *Climate Dynamics*, 46(7), 2391–2402. <https://doi.org/10.1007/s00382-015-2708-9>
- Woollings, T., Li, C., Drouard, M., Dunn-Sigouin, E., Elmetekawy, K. A., Hell, M., et al. (2023). The role of Rossby waves in polar weather and climate. *Weather and Climate Dynamics*, 4(1), 61–80. <https://doi.org/10.5194/wcd-4-61-2023>